No Aging Phenomena in Ferrofluids: The Influence of Coating on Interparticle Interactions of Maghemite Nanoparticles

Ioannis Rabias,* Michael Fardis, Eamonn Devlin, Nikos Boukos, Danai Tsitrouli, and George Papavassiliou

Institute of Materials Science, NCSR Demokritos, 15310 Aghia Paraskeui, Athens, Greece

ARTICLE

ABSTRACT The influence of coating on interparticle interactions in ferrofluids has been investigated using various techniques such as Mössbauer spectroscopy, magnetometry, transmission electron microscopy, photon correlation spectroscopy, X-ray diffraction, X-ray photoelectron, and resonance micro-Raman spectroscopy. Aging and spin-glass-like behavior was investigated in frozen ferrofluids of various concentrations from dense, initial value of 40 mg of coated nanoparticles per 1 mL of water, to dilute 1:10 (4 mg/mL). The as-prepared nanoparticles, core size 7—8 nm, were subsequently coated with a gummic acid corona of 20 nm thickness, which was observed to prevent agglomeration and to delay aggregation even in dense ferrofluids. The resulting separation of magnetic cores due to the coating eliminated all magnetic interparticle interaction mechanisms, such as exchange and dipole—dipole, thus ensuring no aging effects of the magnetic particle system, as manifested in particle agglomeration and precipitation.

KEYWORDS: no aging phenomena · interparticle interactions · ferrofluids · gummic acid · maghemite nanoparticles

Magnetic fluids or ferrofluids are stable colloidal suspensions of ultrafine particles of a ferrite in any ordinary liquid (*e.g.*, water, liquid hydrocarbon, *etc.*).[1] The magnetism of fine particles has been an active field of research for over fifty years.[2] These particles have single domain structures and there is no domain wall present, and a change of the magnetization direction in nanoparticles is not interfered by domain wall movement as is usually the case in bulk magnetic materials.

A popular synthetic method to make single domain particles and prevent agglomeration is the coating of these nanoparticles with appropriate nonmagnetic materials. Such suspensions of coated magnetic nanoparticles have been recently the focus of intensive research not only for the study of the physics of magnetism in the nanometer scale,[3,4] but also for the use of ferrofluids in many technological and biomedical applications such as therapeutic agents for RF-magnetic hyperthermia and as contrast agents in magnetic resonance imaging (MRI).[5−8] MRI contrast agents are chemical substances introduced to the anatomical or functional region being imaged to increase the differences between different tissues or between normal and abnormal tissue, by altering the relaxation times. MRI contrast agents are classified according to the changes in tissue proton-relaxation times they produce after their injection.

To date, gadolinium or manganese salts as well as superparamagnetic iron-oxide-based particles are by far the most commonly used materials as MRI contrast agents.[9] Superparamagnetic contrast agents, as the ones we study, have the advantage of producing an enhanced proton relaxation in MRI better than those produced by paramagnetic ions. Consequently, lower doses are needed which reduce to a great extent the secondary effects in the human body.

Colloidal T2-agents[5] are often called USPIO for ultrasmall superparamagnetic iron oxide, γ-Fe_2O_3. They consist of iron oxide cores, whose composition and physicochemical properties vary continuously from magnetite to maghemite. They are generally synthesized in an one-step process by alkaline coprecipitation of iron(II) and iron(III) precursors in aqueous solutions of hydrophilic macromolecules that serve (i) to limit the magnetic core growth during the synthesis, (ii) to stabilize *via* steric repulsions the nanoparticle dispersion in water (and later in physiological medium), and (iii) to reduce *in vivo* the opsonization process. Such a synthesis allows control of the magnetic core size and size distribution and the overall hydrodynamic diameter, thanks to accurate and reproducible experimental conditions, for example, colloidal stability control, molecular weight, *etc.*

*Address correspondence to irabias@ims.demokritos.gr.

Received for review December 9, 2007 and accepted March 27, 2008.

Published online April 12, 2008.
10.1021/nn700414w CCC: $40.75

This paper discusses the influence of coating on interparticle interactions in ferrofluids and why the basic properties of noninteracting particle systems and thermodynamic perturbation theory which are used to study weakly interacting particle systems do apply in such systems. Aging and spin-glass-like behavior are investigated in frozen ferrofluids in various concentrations from dense, initial value of 40 mg of coated nanoparticles per 1 mL of water, to dilute 1:10 (4 mg/mL). Magnetic nanoparticles of iron oxide coated with gummic acid, a biocompatible macromolecule which easily adsorb on the maghemite surface, were prepared. Gummic acid separates the particles such that no interparticle interaction mechanism could affect them. The particles were obtained by a coprecipitation method, with a mean core size of 7−8 nm and a hydrodynamic size of 25 nm, and successfully dispersed in an aqueous medium giving rise to stable and biocompatible colloidal suspensions. The nature of the nanoparticles as well as the effect of the particle size on the magnetic behavior of the ferrofluid was studied. Techniques of particle characterization such as transmission electron microscopy, Mössbauer spectroscopy, dynamic light scattering, X-ray diffraction, X-ray photoelectron, and resonance micro-Raman spectroscopy and magnetic measurements were used to characterize powder and ferrofluids, and the absolute size values of the particles were analyzed and compared.

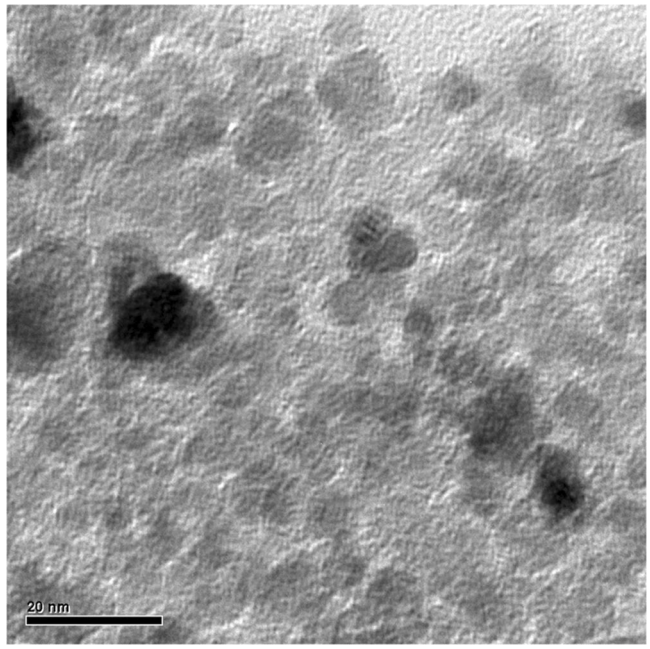

Figure 1. Transmission electron microscopy image of aggregates of gummic-acid-coated USPIO nanoparticles of maghemite (γ-Fe_2O_3). Size was calculated from a sample of 200 particle measurement to be 7 nm.

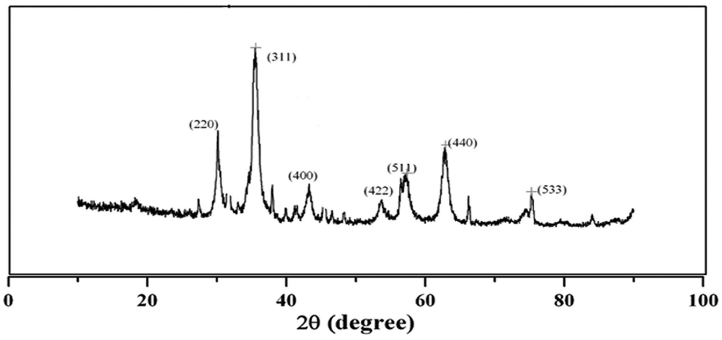

Figure 2. XRD patterns of gummic-coated USPIO nanoparticles of maghemite (γ-Fe_2O_3). Size was calculated by Scherrer formula to be 7−8 nm.

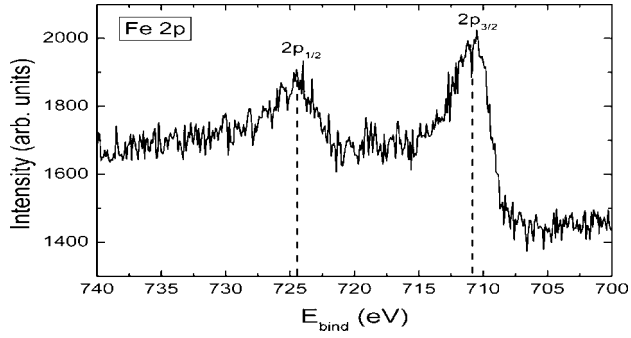

Figure 3. XPS Fe 2p core-level spectra of gummic-acid-coated USPIO nanoparticles of maghemite (γ-Fe_2O_3).

RESULTS AND DISCUSSION

Agglomeration of the USPIO particles is initiated from collisions between the particles during nucleus formation creating clusters in the liquid carrier. Growth of the agglomerate takes place by attractive forces and capillary forces between nascent nucleated clusters and single particles. The cluster size increases until the forces balance between the clusters and equilibrium is reached. USPIO particles have large surface area and small curvature. This large surface energy accelerates the agglomeration process to decrease the free surface energy of the system. To avoid precipitation of USPIO, stabilization is introduced against agglomeration using polysaccharide molecules such as gummic acid.

In Figure 1, one can observe the TEM image of aggregates, due to evaporation of the water in the procedure, of coated ultrasmall iron oxide nanoparticles. Owing to its amorphous structure, gummic acid cannot be seen but is affecting the low standard deviation in the size of these particles which is clearer in the DLS data in Figure 4.

In Figure 2, XRD powder patterns of iron oxide phases allow the identification of a major cubic spinel phase. This indicates the presence of maghemite γ-Fe_2O_3 with an average size of 7−8 nm (space group $P4_132$). Figure 3 shows the XPS spectra of the γ-Fe_2O_3 in the Fe 2p core-level region. The background has been subtracted using the Shirley method, the electron take-off angle has been adjusted to 45° with respect to the surface normal. Two weak but well-defined peaks at approximately 710.8 and 724.2 eV, are observed, in agreement with the typical values of the Fe $2p_{3/2}$ and $2p_{1/2}$ core-level XPS peaks for ferric oxides.[13,14] In addition,

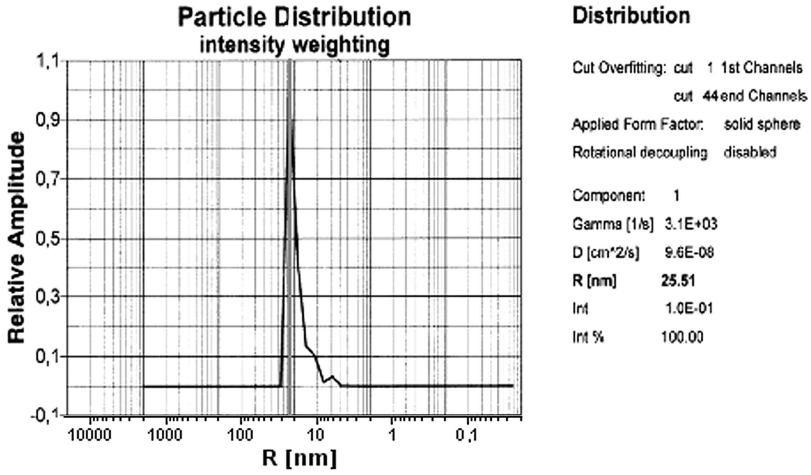

Figure 4. Gummic-acid-coated USPIO nanoparticles of maghemite (γ-Fe_2O_3) log-normal particle distribution by DLS.

the main Fe $2p_{3/2}$ and $2p_{1/2}$ peaks are accompanied by weak satellite structures on their high binding energy side, about 8 eV above the respective Fe 2p line. Such a spectrum is typical of Fe_2O_3 oxides (α- and γ-Fe_2O_3 polymorphs).[13,14]

The hydrodynamic size from dynamic light scattering data, Figure 4, was $R = 25$ nm using the intensity weighting distribution technique showing a single narrow peak, a sign of monodisperse nanoparticles. The macroscopic magnetic moment of the coated magnetic nanoparticles was measured at room temperature as a function of the magnetic field using a vibrating sample magnetometer with the applied field varying between $\pm$ 20 kOe. The magnetization data for the gummic-acid-coated nanoparticles are shown in Figure 5.

Assuming that the sample consists of noninteracting single-domain particles, in the superparamagnetic state, the magnetization is described by the Langevin function:[17]

$$L\left(\frac{\mu \mathbf{H}}{k_B T}\right) = \coth\left(\frac{\mu \mathbf{H}}{k_B T}\right) - \frac{\mu \mathbf{H}}{k_B T} \qquad (1)$$

where μ is the magnetic moment of a particle, **H** is the applied field, and k_B is the Boltzmann constant. Since inevitably there will be a distribution of the sizes of the magnetic particles, it is customary practice[18] to introduce a distribution function of the magnetic moments $f(\mu)$, and the magnetization $\mathbf{M}(H, T)$ is then described by

$$\mathbf{M}(\mathbf{H}, T) = \int_0^\infty \mu L\left(\frac{\mu \mathbf{H}}{k_B T}\right) f(\mu)\, d\mu \qquad (2)$$

The magnetization data **M** plotted as a function of 1/**H** are shown in Figure 5. The saturation magnetization $\mathbf{M}_s = N\langle\mu\rangle$ thus obtained was found to be $\mathbf{M}_s$ = 12.6 emu/gr much lower than the corresponding one for the bulk maghemite (50 emu/gr), a reduction frequently encountered in the literature.[5] The USPIO are ferri- or ferromagnetic single domain particles that have an anisotropy energy barrier of the same order as the thermal energy. Reduced magnetization in small ferrite particles compared to the bulk is well documented in the literature, but the nature of the spin structure in such particles has not been well understood. Proposed mechanisms for moment reduction include shell−core structures, spin canting, spin-glass behavior *etc.*[5]

Using the initial slope of the magnetization data in Figure 5, the saturation magnetization and the moments of the log-normal distribution function, the following statistical parameters for the magnetization were obtained: $\mu_0 = 1239\ \mu_B$, $\langle\mu\rangle = 2707\ \mu_B$, $\sigma = 1.25$, and $N = 5.02 \times 10^{17}$/g. The mean magnetic moment $\langle\mu\rangle = 2707\ \mu_B$ corresponds to a mean particle diameter $\langle d\rangle_{magn} = 5$ nm, if $I_s = 500$ emu/cm^3 is assumed for the saturation magnetization of bulk maghemite.[5] This magnetically derived mean particle diameter $\langle d\rangle_{magn} = 5$ nm, is somewhat smaller than the one derived from TEM images and XRD data (Figures 1, 2). This difference is frequently encountered in the literature and may be due to the presence of a magnetic dead layer around the particle, resulting in a magnetic particle volume derived from magnetization data smaller than the crystalline core volume.[6] Also, some of the iron oxide species may exist as a nonmagnetic amorphous phase, which does not contribute to

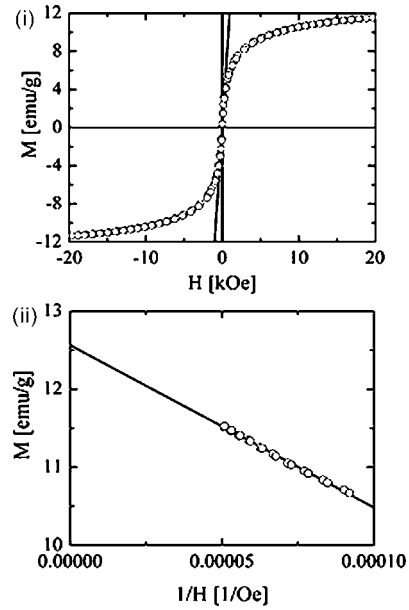

Figure 5. (i) Magnetization for dry powder sample of coated nanoparticles. The solid line is a linear fit to the low field data near the origin. (ii) Magnetization data near saturation, as a function of 1/H.

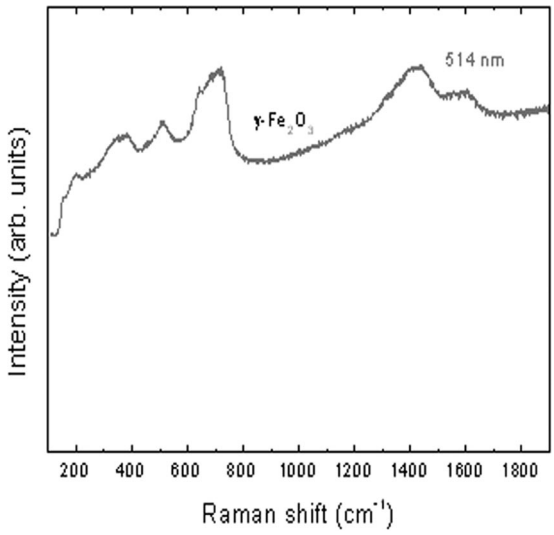

Figure 6. Resonance micro-Raman spectra of gummic-acid-coated nanoparticles of γ-Fe_2O_3 at excitation wavelength of 514 nm (vis).

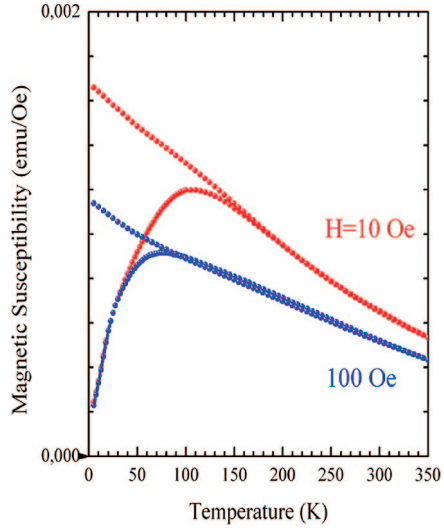

Figure 7. Magnetic susceptibility χ curves taking in FC and ZFC modes of gummic acid coated maghemite nanoparticles at $\mathbf{H} = 10$ and 100 Oe.

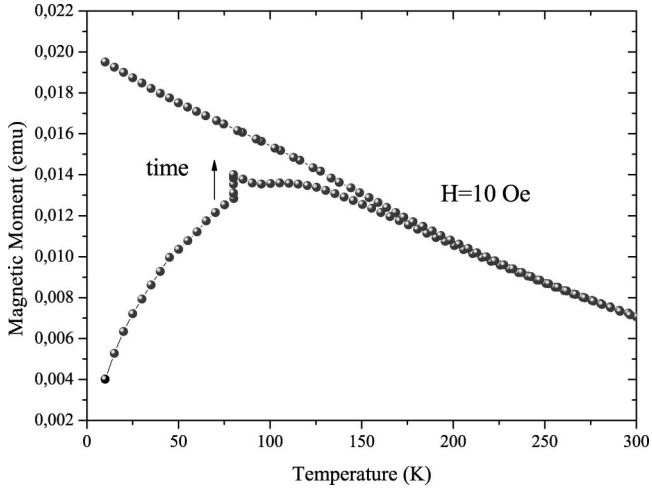

Figure 8. Magnetization curves taking in FC and ZFC modes of gummic-acid-coated maghemite nanoparticles at $\mathbf{H} = 10$ Oe, measurement temperature T_m at 77 K, and wait time of $t_w = 10^4$ s.

the magnetic behavior, or as an iron phase that will have a smaller effect on magnetization than a maghemite only phase.

The Raman spectrum in Figure 6 occurs at the excitation wavelength of 514 nm, where several broad bands extending up to high wavenumbers appear. Specifically, three broad bands around 350, 510, and 700 cm^{-1} emerge. They are a characteristic feature of the iron-deficient spinel phase of γ-Fe_2O_3,[15] along with two higher frequency broad bands at 1420 and 1600 cm^{-1}, frequently observed in maghemite as well, though possibly related to carbonaceous species.[16]

The influence of coating on interparticle interactions were investigated by experimental techniques such as zero-field-cooled (ZFC)/field-cooled (FC) magnetization techniques using superconducting quantum inteference device (SQUID) magnetometry and Mössbauer spectroscopy. Our coated nanoparticles were placed in a SQUID magnetometer and cooled in zero-field from room temperature to 4.2 K. In Figure 7, the magnetic susceptibility χ *versus* temperature T in $\mathbf{H} = 10$ and 100 Oe was plotted. The lower curve (ZFC) both in 10 and 100 Oe was obtained by cooling the system in zero magnetic fields from 300 to 4.2 K.

The magnetic field **H** was then applied and magnetization was measured as temperature was increased in both cases. The upper curve (FC) was obtained by cooling the system but now in the measuring field. As the sample was warmed up slowly, the energy barriers in some of the nanoparticles started to be overcome by thermal activation energy, k_{BT}, and these nanoparticles achieved a superparamagnetic state. When the relaxation time τ of these nanoparticles exceeded the SQUID measuring time of 10 s, the magnetization of these nanoparticles was no longer observed by the SQUID and the total magnetization of the sample decreased.

The maximum of the ZFC curve was related to the blocking temperature and was located at $T_B = 80$ K for $\mathbf{H} = 100$ Oe and 110 K for 10 Oe, respectively, as one could expect for superparamagnetic nanoparticles.[19] FC and ZFC branches were merged at higher temperatures for $\mathbf{H} = 100$ Oe at around 90 K and for 10 Oe at 160 K. The peak in the ZFC curve was field dependent as shown in Figure 7. The T_B value was decreased as well as the distance between the merging of the ZFC and FC curves as H was increased. The application of an external field apparently decreases the barriers to spin reorientation. For a larger field $\mathbf{H} = 1000$ Oe, one could expect the magnetic energy to dominate the interaction energy.

To investigate if interparticle interactions impose aging effects in coated frozen ferrofluids, time dependent magnetization measurements for the most concentrated coated sample, 10% by volume, were performed. In Figure 8, the sample was cooled in zero field to the measurement temperature T_m, in this case 77 K. After a wait time $t_w = 10^4$ s at $T_m = 77$ K and a magnetic field

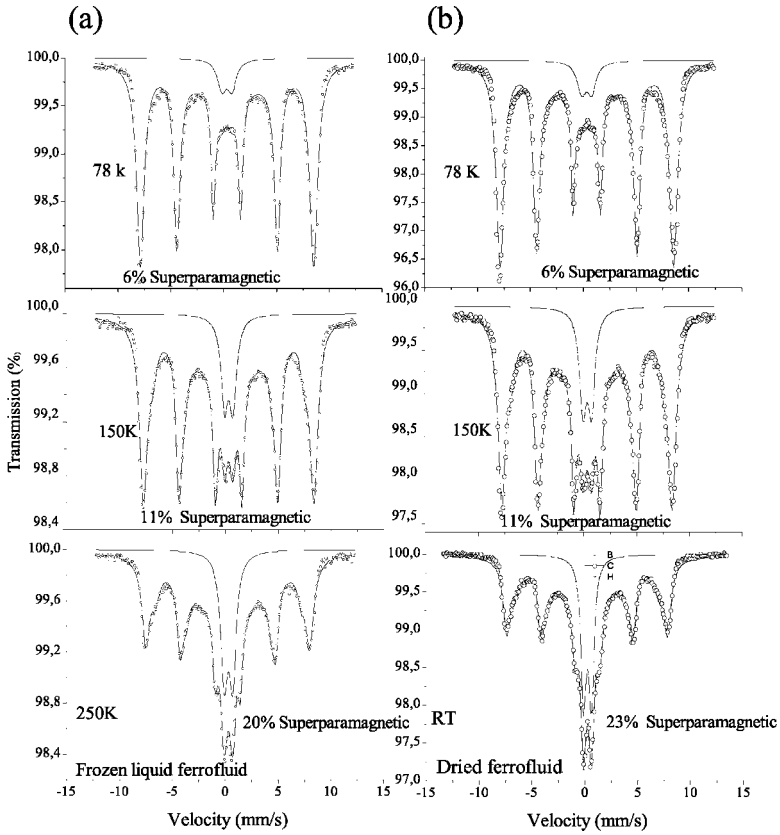

Figure 9. Mössbauer spectra of (a) dense frozen ferrofluid, concentration 40 mg/mL, and (b) dry powder samples of gummic-coated maghemite nanoparticles at 78, 150, and 250 K and room temperature.

H = 10 Oe, it is clearly observed that the relaxation is independent of the wait time and no aging phenomena appear. The relaxation is only governed by dynamics of individual coated nanoparticles and the same applies to the more diluted samples.

The behavior of the ZFC and FC susceptibility of gummic acid coated maghemite nanoparticles gives an insight into the low temperature dynamics of magnetic moments of superparamagnetism. The phase diagrams for gummic acid coated maghemite nanoparticles could be explained as follows. T_c is defined as the Curie temperature and for $T > T_c$, the spins inside each nanoparticle are randomly distributed and the particles behave paramagnetically. For $T_b < T < T_c$, the spins inside each nanoparticle are ferrimagnetically ordered; they form a single ferrimagnetic domain. In this superparamagnetic phase, each domain consisting of a number of spins coupled magnetically behaves like a single superspin and is characterized by a net magnetic moment, **M**. There is either negligible or no interaction between each such domain. This can be ascertained by the absence of hysteresis above T_b. The thermal activation energy and anisotropy energy are the only source of perturbation, there is negligible interaction between the ferrimagnetic particles. With decrease in temperature $T < T_b$, the net spin of each cluster eventually aligns with the anisotropy axis and gets frozen into what is known as the "blocked" state.

The Mössbauer spectra were obtained using a conventional constant acceleration spectrometer with a source of ^{57}Co in rhodium metal. The magnetically split spectrum at 78 K is typical of maghemite and a slight asymmetry was observed in both the line width and the intensity because of the small difference in the parameters of the two iron sites in the spinel structure. Spectra of the frozen gummic-acid-coated maghemite ferrofluid at temperatures between 78 and 250 K, and of the dried powder sample of the same material at temperatures between 78 and 300 K, are shown in Figure 9a and 9b, respectively. As one could expect, spectra show a slow but gradual transition from a six-line magnetically split spectrum to a superparamagnetic doublet.[20]

The coating is influencing the interparticle interactions of the nanoparticles and the blocking temperature, which is defined as the temperature at which a particle with volume equal to the median of the volume distribution has a relaxation time of the order of the time scale of Mössbauer spectroscopy, $\tau_m \approx 5 \times 10^{-9}$ s, Figure 9. Within experimental error no difference between the spectra of the coated nanoparticles in suspended and dry form is detected. The spectra of the coated samples show the presence of both a quadrupole doublet and a six-line component in a broad temperature range. Also by comparing the spectra of differently diluted samples of frozen ferrofluids from dense, initial value of 40 mg of coated nanoparticles per 1 mL of water, to dilute 1:10 (4 mg/ml), we show that the interparticle interaction causes no aging effect in coated nanoparticles.

The Mössbauer spectra of Figure 10 were measured after sonication, at 150 K, of 1:10 diluted ferrofluid (4 mg/ml) of gummic-acid-coated nanoparticles. They present little difference from the spectra of Figure 9a, also measured at 150 K, proving that the coating protects the particles from agglomerating in dense and diluted environment.

CONCLUSIONS

The nature of the nanoparticles, as well as the effect of the particle size on the magnetic behavior of the ferrofluid has been studied. The TEM, XRD, XPS,

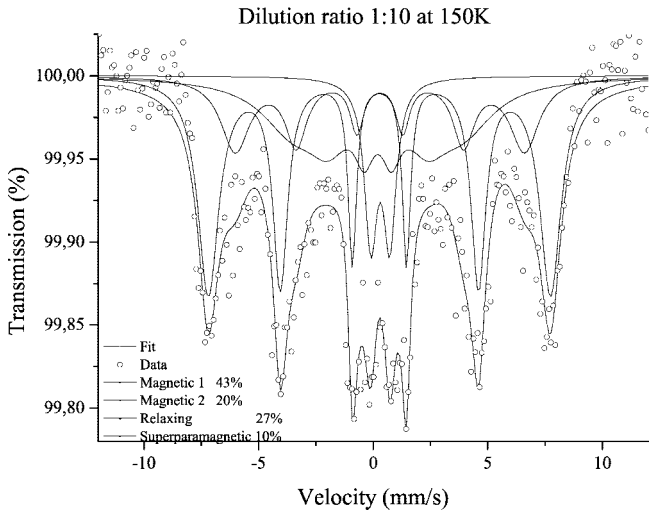

Figure 10. Mössbauer spectra of frozen ferrofluid of gummic-acid-coated maghemite nanoparticles in dilution ratio of 1:10, concentration at 4 mg/mL, at 150 K.

and DLS characterization techniques and VSM, SQUID, and Mossbauer magnetic measurements showed that the particles exhibited a superparamagnetic behavior as expected for nanometer-sized particles with an average magnetic core diameter of 7−8 nm and a hydrodynamic core of $R = 25$ nm. First we have measured ZFC and FC susceptibility χ of gummic-acid-coated maghemite nanoparticles as a function of temperature; the susceptibility was characterized by an increase in χ (FC) below T_b with decreasing temperature. Measurements of magnetization with and without a waiting time of 10^4 s were also showing superparamagnetic character of the densest ferrofluid, of 40 mg of coated nanoparticles per 1 mL of water, proving that the influence of gummic acid coating leads to no detectable interparticle interaction. Second the Mössbauer spectra of gummic-acid-coated maghemite nanoparticles at 150 K from 40 to 4 mg/ml of frozen ferrofluids as well as powders showed no difference. Thus, aging, memory, and rejuvenation effects are not observed, leading to the conclusion that gummic acid is effective in preventing agglomeration and exchange interaction. Thus, this ferrofluid, after biocompatibility and cytotoxicity tests, could be a promising candidate for a future MRI contrast agent applications.

METHODS

Particle Preparation. A dispersion of USPIO nanoparticles coated with gummic acid was synthesized by the reaction of ferric chloride and ferrous chloride in the presence of ammonia, using a coprecipitation method.[10,11] Gum arabic is generally accepted to be a mixture of salts of calcium, magnesium, and potassium formed by the union of these elements with gummic acid. The gum is chiefly composed of calcium arabate. Gummic acid forms salts containing an excess of acid. It is considered identical with the metapectic acid of Frémy and is obtained from a solution of the gum, acidulated with chlorhydric acid, by precipitation with alcohol. Before drying gummic acid is soluble in water, but after drying it becomes metagummic acid, and refuses to dissolve in either hot or cold water unless alkalinized. The nominal molecular weight of the gummic acid used was 250 000. Gummic-acid-coated maghemite nanoparticles were prepared by coprecipitation of a mixture of 50 mL of aqueous solutions (0.66 M $FeCl_3$ and 0.33 M $FeCl_2$). This mixture was added, under constant stirring on a magnetic stir plain, dropwise over 1 min to a 50 mL alkaline solution of NaOH (1 M) that contained 1 wt % of gummic acid. The stirring continued for 20 min under a nitrogen-gas atmosphere. The particles obtained were washed three times with ethanol and water using ultracentrifugation (5000 rpm for 10 min at 10 °C) with nitrogen-purged water. The coated iron oxide nanoparticle yield, determined by weighing of the lyophilized sample of the preparation, was 400 mg. Formulations of iron oxide nanoparticles were developed, first by optimizing the amount of gummic acid coating required to coat iron oxide nanoparticles completely, and then by optimizing the amount of coating required to form an aqueous dispersion of polysaccharide-coated nanoparticles. The formulations were heated to 60 °C while being stirred for 30 min and then cooled to room temperature. The black precipitate thus obtained was washed twice with 10 mL of water. The precipitate was lyophilized for 2 days at −60 °C and dispersed in 10 mL of water. Finally, the colloidal suspension was filtered through a 0.22 μm pore size filter yielding a 40 mg/ml ferrofluid that was stable for more than 1 year. For the purpose of the experiment this ferrofluid with the initial value of 40 mg of coated nanoparticles per 1 mL of water was diluted by 1:2 (20 mg/ml) and 1:10 (4 mg/ml).

Characterization Techniques. Dry powders and aqueous suspensions of the coated magnetic nanoparticles were prepared and subsequently characterized by a number of techniques including transmission electron microscopy, dynamic light scattering, X-ray diffraction, X-ray photoelectron, VSM magnetometry, Mössbauer spectroscopy, and resonance micro-Raman spectroscopy.

Crystallographic analysis of the samples was carried out from the X-ray diffraction patterns, recorded between 20° to 100° (2θ) at 0.5° min^{-1} in a Siemens D500 diffractometer with Cu Kα radiation. X-ray tube voltage and current were set at 40 kV and 35 mA, respectively. The crystallite size was obtained from the full width half-maximum of the (311) reflection typical for iron oxide using the Debye−Scherrer equation.[12]

Using photon spectroscopy, dynamic light scattering measurements of gummic-acid-coated USPIO nanoparticles were performed by a Microtrac series 9200 ultrafine particle analyzer. Results were reported as the mean intensity-weighed particle size.

For the transmission electron microscopy analysis, a 200 keV Phillips CM20 microscope was used to observe the morphology, mean size, and distribution of the nanoparticles in the powder, and the mean aggregate size in the colloidal suspensions. This determination was made on a large number, by measuring at least 200 particles, from different micrographs. The specimen for TEM imaging was prepared from the USPIO suspension in deionized water by using sonication for 3 min. The colloidal suspensions were highly diluted and nebulized onto the microscope grid to avoid particle agglomeration during the preparation of the samples. After sonication, 1 mL of the USPIO suspension was centrifuged for 5 min at 14 000 min^{-1}. A drop of well-dispersed supernatant was placed on a carbon-coated 200 mesh copper grid, followed by drying the sample at ambient conditions before it was attached to the sample holder on the microscope. The mean size measured by electron microscopy corresponds to the magnetic core of the aggregates.

Acknowledgment. The authors are thankful to the Greek General Secretariat for Research and Technology for providing financial support though National Projects, EPAN(YB-23) and PEP Attikis (ATT-25).

Supporting Information Available: Figure S1, gummic-acid-coated USPIO nanoparticles of maghemite (γ-Fe_2O_3) linear particle distribution by DLS; and Figure S2, gummic-acid-coated USPIO nanoparticles of maghemite (γ-Fe_2O_3) linear core size distribution by TEM. This material is available free of charge *via* the Internet at http://pubs.acs.org.

REFERENCES AND NOTES

1. Dormann, J. L.; Fiorani, D.; Tronc, E. Magnetic Relaxation in Fine-Particle Systems. *Adv. Chem. Phys.* **1997**, *98*, 283–494.
2. Néel, L. Theorie du Trainage Magnetique des Ferromagnetiques en Grains Fins avec Applications aux Terres. *Ann. Geophys.* **1949**, *5*, 99–136.
3. Dormann, J. L.; Bessais, L.; Fiorani, D. A Dynamic Study of Small Interacting Particles: Superparamagnetic Model and Spin-Glass Laws. *J. Phys. C. Solid State Phys.* **1988**, *21*, 2015–2034.
4. Kodama, R. H. Magnetic Nanoparticles- Condens. Matter. *J. Magn. Magn. Mater.* **1999**, *200*, 359–372.
5. Hergt, R.; Hiergeist, R.; Zeisberger, M.; Glöckl, G.; Weitschies, W.; Ramirez, L. P.; Hilger, I.; Kaiser, W. A. Enhancement of AC-Losses of Magnetic Nanoparticles for Heating Applications. *J. Magn. Magn. Mater.* **2004**, *280*, 358–368.
6. Shinkai, M. Functional Magnetic Particles for Medical Application. *J. Biosci. Bioeng.* **2002**, *94*, 606–613.
7. Van Beers, B. E.; Sempoux, C.; Materne, R.; Delos, M.; Smith, A. M. Biodistribution of Ultra Small Iron Oxide Particles in the Rat Liver. *J. Magn. Reson. Imaging.* **2001**, *13*, 594–599.
8. Roberts, T. P. L; Chuang, N.; Roberts, H. C. Neuroimaging: Do We Really Need New Contrast Agents for MRI. *Eur. J. Radiol.* **2000**, *34*, 166–178.
9. Berry, C. C.; Curtis, A. S. G. Functionalization of Magnetic Nanoparticles for Applications in Biomedicine. *J Phys D: Appl Phys.* **2003**, *36*, 198–206.
10. Massart, R.; Cabuil, V. Synthese en Milieu Alcalin de Magnetite Colloidale: Contrôle du Rendement et de la Taille des Particules. *J. Phys. Chem.* **1987**, *84*, 967–973.
11. Granqvist, C. G.; Buhrman, R. H. Ultra Fine Particles. *J. Appl. Phys.* **1976**, *47*, 2200–2219.
12. Klug, H. P.; Alexander, L. E. *X-Ray Diffraction Procedures: For Polycrystalline and Amorphous Materials*; Wiley-VCH: New York, 1974; 992.
13. McIntyre, N. S.; Zetaruk, D. G. X-Ray Photoelectron Spectroscopic Studies of Iron Oxides. *Anal. Chem.* **1977**, *49*, 1521–1529.
14. Fujii, T.; De Groot, F. M. F.; Sawatzky, G. A.; Voogt, F. C.; Hibma, T.; Okada, K. *In Situ* XPS Analysis of Various Iron Oxides Films Grown by NO_2-assisted Molecular-Beam Epitaxy. *Phys Rev. B* **1999**, *59*, 3195–3202.
15. Bersani, D.; Lottici, P. P.; Montenero, A. Micro-Raman Investigation of Iron Oxide Films and Powders produced by Sol-Gel Syntheses. *J. Raman Spectrosc.* **1999**, *30*, 355–360.
16. Chourpa, I.; Douziech-Eyrolles, L.; Ngaboni- Okassa, L.; Fouquenet, J. F.; Cohen-Jonathan, S.; Souce, M.; Marchais, H.; Dubois, P. Molecular Composition of Iron Oxide Nanoparticles, Precursors for Magnetic Drug Targeting, as characterized by Confocal Raman Microspectroscopy. *Analyst* **2005**, *10*, 1395–1403.
17. Cullity, B. D. *Introduction to Magnetic Materials; Assison-Wesley: Reading* **1972**, 89–109.
18. Ferrari, E. F.; Da Silva, F. C. S.; Knobel, M. Influence of the Distribution of Magnetic Moments on the Magnetization and Magneto Resistance in Granular Alloys. *Phys. Rev. B.* **1997**, *56*, 6086–6093.
19. Lierop, J. V.; Ryan, D. H. Moessbauer Spectra of Ferrofluids Characterized Using a Many State Relaxation Model for Superparamagnets. *J. Appl. Phys.* **2000**, *87*, 6277–6279.
20. Mörup, S.; Tronc, E. Superparamagnetic Relaxation of Weakly Interacting Particles. *Phys. Rev. Lett.* **1994**, *72*, 3278–3281.